Available online at www.sciencedirect.com
SCIENCE DIRECT
Polymer 46 (2005) 7109–7117
polymer
www.elsevier.com/locate/polymer

Phase separation in randomly charged polystyrene sulphonate ionomer solutions

Edoardo De Luca[a], Thomas A. Waigh[a,*], Joon Seop Kim[b], Ho Seung Jeon[b], Wim Pyckhout-Hintzen[c]

[a]*Polymers and Complex Fluids, School of Physics and Astronomy, University of Leeds, Leeds, LS2 9JT, UK*
[b]*Department of Polymer Science and Engineering, Chosun University, Kwangju, South Korea*
[c]*Institut für Festkörperforschung, Forschungszentrum Jülich, Jülich, Germany*

Received 21 September 2004; received in revised form 1 March 2005; accepted 9 May 2005
Available online 21 June 2005

Abstract

The dynamics of randomly charged polystyrene caesium–sulfonate ionomers in semi-dilute solutions were studied using a combination of dynamic light scattering (DLS), small angle neutron scattering (SANS), and bulk rheology. The samples were studied in toluene solutions where the aggregation of the dipolar groups is favoured. Evidence of aggregation in dilute solution is found using DLS and SANS with both the hydrodynamic and static radius of gyration indicating that there is a contraction of the chains due to intra-chain attractive forces. SANS experiments demonstrate the evolution of the aggregates into a network structure as a function of polymer concentration. The association process is caused by the dipolar attraction between the charged groups and introduces two static correlation lengths in the mesh structure of the network; the standard semi-dilute mesh size ($\xi = 1.12c^{-0.72\pm0.03}$) and an inhomogeneity length ($\Xi = 24c^{0.58\pm0.05}$) due to micro-phase separation. The scaling of the amplitudes of the correlation lengths $I_1(0) \sim c^{-0.33\pm0.07}$ and $I_2(0) \sim c^{2.0\pm0.4}$ are consistent with good solvent conditions and micro-phase separation, respectively. An imposed shear causes the break up of the micro-phase separated micellar system with a characteristic yield stress for the Bingham step-like shear thinning.

Keywords: Gelation; Yield stress; Polystyrene caesium sulfonate

1. Introduction

Ionomers are generally non-polar polymers containing small amounts, usually less than a 5% fraction of covalently bound salt molecules, which are present as side or end groups. The aggregation of ionomers in non-polar media has been a subject of investigation for several years and it is known that the association of salt groups can result in the formation of intra- and inter-chain aggregates in non-polar solvents [1]. Furthermore, in the solid state these aggregates form microscopically separated domains. The aggregates are physically cross-linked, an arrangement that dominates the major properties of such polymers in non-polar media and gives rise to the application of ionomers as thermoplastics, surface-active materials, and oil viscosity modifiers [2,3].

The study of ionomer aggregation in non-polar solvents is much less advanced than that of ionomers in the solid state, because their poor solubility restricts the samples to those having a very low content of salt groups, typically 1–4 mol%. Lundberg and co-workers have studied ionomer aggregation of polystyrene sulfonate (PSS) ionomers in various non-polar solvents [4]. A cross-over behaviour has been observed in the concentration dependence of the reduced viscosity attributed to a change between intra- and inter-molecular association. At low concentrations the reduced viscosity for the ionomers was found to be smaller than that for unsulphonated polystyrene, and, with an increase of ionomer concentration, the viscosity increases drastically exceeding that of the polystyrene [5,6]. The results suggest that an intra-to inter-chain associating equilibrium determines the viscosity of the unmodified

* Corresponding author. Address: Department of Physics and Astronomy, University of Leeds, Leeds, LS2 9JT, UK. Tel.: +44 113 3433849; fax: +44 113 3433846.
E-mail address: t.a.waigh@leeds.ac.uk (T.A. Waigh).

0032-3861/$ - see front matter © 2005 Elsevier Ltd. All rights reserved.
doi:10.1016/j.polymer.2005.05.096

ionomer solutions. Recent data of both small angle neutron and light scattering have shown the presence of intra- and inter-chain aggregates in ionomer solutions [1]. It has been demonstrated [7–9] using light scattering that the single-chain dimension of the sodium salt of PSS ionomer with 1.39 mol% salt groups at their lowest concentration (0.045 g dl^{-1}) in xylene was approximately 20% smaller than the single-chain dimension of the unmodified polystyrene in the same solvent. This contraction has been attributed to the intra-chain association of individual ionomer coils in the dilute regime.

Static thermodynamic gelation and phase separation have been observed previously for PSS in decalin [10] and static scattering studies of gelling polymeric species has a long history [11]. Polystyrene solutions in good solvents have a semi-dilute mesh structure which is well described by scaling theory [12], but an additional excess scattering is often detected at large length scales. This is less well understood and has been attributed to frozen blob inhomogenieties in the polymeric network [11].

Dynamic scaling theories have recently been applied to polymer solutions with random sticker functionalities [13,14] and a series of predictions for the rheology have been made, showing reasonable agreement with experiment. PSS ionomers in the solid state have demonstrated sticky reptation dynamics with ion beam analysis studies [15] and long-range inhomogeneities have been observed using ultra low-angle X-ray scattering [16].

We investigated the aggregation process in PSS ionomer solutions using scattering techniques such as dynamic light scattering (DLS) and small angle neutron scattering (SANS). Furthermore, we examine the evolution of the inter- and intra-chain associations with polymer concentration and their consequent effect on rheological properties. Static scattering techniques allow gelling polymeric solutions to be loosely categorised as types 1, $1'$,$1'+I$ and 2 [11]. In the present article, we study associating polymers with SANS profiles typical of type $1'+I$ gels formed by physical dipolar cross-links. These are heterogeneous polymeric networks with large scale inhomogeneities. Other examples of gels with similar SANS profiles to the PSS ionomers include chemically linked specimens such as polydimethylsiloxane networks in octane [17] and amino-methylated polystyrene [18]. Shear induced macro phase separation has been found in a number of complex fluid systems [19,20]. We present evidence of such phenomenon for the first time in randomly charged ionomer solutions.

2. Experimental section

2.1. Materials

Polystyrene samples (M_w = 55,000, 87,000, and 158,000 g mol^{-1}; polydispersity was 1.55 for all the samples with no important variation after the sulfonation) were prepared by bulk free-radical polymerization using benzoyl peroxide as initiator. For homogeneous sulfonation, the method developed by Makowski et al. [21] was used to obtain the poly (styrene-*co*-styrenesulfonic acid) samples. To determine the acid content, the samples were dissolved in a benzene/methanol (9/1 v/v) mixture to make a 5% (w/v) solution, and titrated with standard methanolic NaOH to the phenolphthalein end point. The neutralization of the acid groups was performed by the addition of predetermined quantity of methanolic CsOH solution to a 5% (w/v) acid copolymer solution in a toluene/methanol (9/1 v/v) mixture. The concentration of the polymers in solution is reported in moles of monomer per litre of solution (M). The ionomers were dissolved in toluene in all of the experiments. All of the samples examined corresponded to about 1% sulfonation.

2.2. Dynamic light scattering

An ALV 5000 goniometer was used with a fast correlator (10 ns) and a 100 mW argon ion laser. The apparatus was tested with respect to a series of standard polystyrene colloids in toluene. The PSS-Cs samples were dissolved in toluene and filtered with 0.45 μm PTFE membrane filters before the analysis. Intensity correlation functions were measured in the angular range 30–140° and for polymer concentrations in the range 0.0047–0.47 M. The dynamic light scattering data were analyzed by inverse Laplace transformation using the CONTIN [22] method. This yields a distribution function of decay rate, Γ, $G(\Gamma, q)$, defined Eq. (1).

$$g_1(q,t) = \int_0^\infty G(\Gamma, q)\exp(-\Gamma t)\mathrm{d}\Gamma \tag{1}$$

where $g_1(q,t)$ is the normalized electric field autocorrelation function at delay time t and scattering vector $\boldsymbol{q}$ defined as $\boldsymbol{q} = (4\pi n_0/\lambda_0)\sin(\theta/2)$, where n_0 is the refractive index of the solvent, λ_0 is the wavelength of the incident light in vacuum (488 nm) and θ is the scattering angle. Experimentally, the normalized intensity autocorrelation function, $g_2(q, t)$, is measured first, which can then be converted to the electric field autocorrelation function, $g_1(q,t)$, via Eq. (2).

$$g_2(q,t) = B\left[1 + b|g_1(q,t)|^2\right] \tag{2}$$

where B is the baseline and b is an optical constant. The value of B is obtained from the long time delay channels of the composite correlation function.

In the case of simple diffusion, the angular dependence of the decay rate can be described by $\Gamma/q^2 = D_{App}$, where D_{App} is the apparent diffusion coefficient of the polymer for the specific concentration. The decay times calculated by the use of CONTIN were transformed into Γ and the plot of the latter against q^2 gave the D_{App} that provided a diffusion coefficient D_0, by the extrapolation to zero concentration. The spectrum of the decay rate obtained by CONTIN

analysis produced a series of distinct peaks, each corresponding to a different relaxation process.

2.3. Small angle neutron scattering (SANS)

SANS experiments were carried out at FRJ-2, Forschungszentrum Jülich (Jülich, Germany) using the spectrometer KWS1 (http://www.fz-juelich.de/iff/wns_kws1). The samples to detector distances used were 2 and 8 m with an incident beam diameter of 10 mm. The two camera lengths provided $\lambda = 7$ Å, a wavelength spread ($\Delta\lambda/\lambda$) of 20% and a q-range of 0.02–0.16 $Å^{-1}$ (39–314 Å in real space). The ionomer samples were dissolved in deuterated toluene 48 h before the experiments and the concentration range was 0.0943–2.83 M. The sample thickness was 2 mm.

Standard procedures of data treatment were used. The detector sensitivity and the transformation to absolute scattering (cm^{-1}) were achieved pixel wise by calibrating to the scattering of a secondary Lupolene standard at the same collimation conditions and solid angle. The transmission was monitored in situ using the attenuated direct beam through the middle of the semi-transparent beam stop. The absolute scattering intensity was obtained by subtracting off the appropriate scattering of the empty cell, electronic and gamma background.

2.4. Bulk rheology

Shear rheometry experiments were performed using a Bohlin CVO with an ultra small Couette cell geometry (cone angle of 1°, radius of 20 mm and gap 0.07 mm). The samples were loaded gently into the Couette cell by a pipette and allowed to equilibrate for a few minutes before each measurement. Measurements were conducted at 25 °C. To minimize the effects of solvent evaporation a solvent trap with a toluene reservoir was used. Measurements of the dynamic shear moduli were conducted in the frequency range 0.1–100 Hz and all the measurements were obtained at frequencies and strains where a linear response was verified.

3. Results and discussion

3.1. Dynamic light scattering

In ionomer solutions with non-polar solvents the majority of the counter-ions are thought to be associated with the polymer backbone, forming ion pairs that interact with each other in molecular aggregates [3]. The bimodal correlation curves (Fig. 1) analysed by CONTIN showed two diffusive modes, with the relaxation rate scaling as q^2 in both cases. The fast mode gave a diffusion coefficient (D_f), on the order of 10^{-7} cm^2/s attributed to the motion of single chains, and the slow mode with a diffusion coefficient (D_s), on the order of 10^{-8} cm^2/s, was thought to reflect the motion of the aggregates. This is in agreement with a study of Body comb and Hara on sodium-sulfonated polystyrene [23] in a polar solvent (DMF).

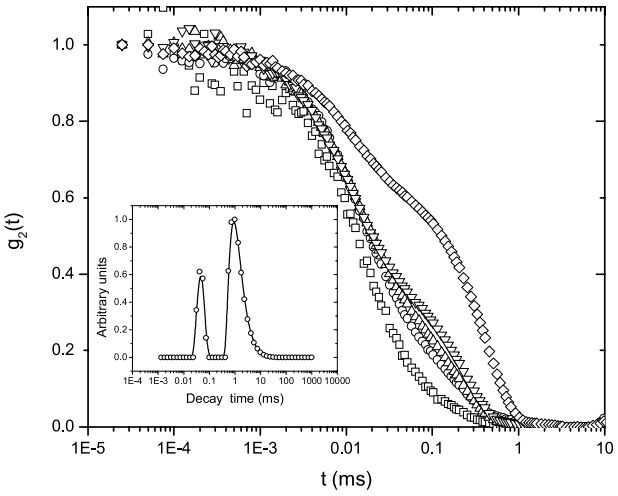

Fig. 1. Correlation function $g_2(t)$ as function of relaxation time for PSS-Cs ($M_w = 87{,}000$ g mol^{-1}) collected at 90° in a range of concentrations of 0.094–0.47 M. Inset: example of CONTIN analysis showing the fast and slow mode due to the single chain and the aggregate dynamics, respectively.

Another issue of interest is the scaling of the hydrodynamic radius (R_h) of the single chain with the molecular weight. R_h can be calculated from the diffusion coefficient in the limit of zero polymer concentration (D_0)

$$R_h = \frac{kT}{6\pi\eta_0 D_0} \tag{3}$$

where kT is the thermal energy, and η_0 is the solvent viscosity.

In our experiments, we found with PSS that the hydrodynamic radius scaled with the degree of polymerisation N as $R_h \sim aN^{0.48\pm0.02}$. Theory gives $R_h \sim aN^{1/2}$ for unsulfonated polystyrene in a theta solvent [24], but the agreement with our results is only coincidental, they are better explained by a contraction of the unsulphonated result in a good solvent, $R_h \sim aN^{3/5}$ due to interchain association [13]. For polystyrene in toluene the scaling exponent for R_h was found to be equal to -0.577 in previous DLS experiments [25] i.e. $R_h \sim N^{0.577}$. A similar contraction of the hydrodynamic radius ($\sim$25%) due to the dipolar interactions has been observed previously with ionomer solutions [1].

Pedley and co-workers [7] studied sodium-sulfonated polystyrene in xylene solutions by static and dynamic light scattering. The extent of aggregation via intermolecular ion pair interactions was determined by a chemical equilibrium between single contracted chains and multichain clusters. They explained the data in terms of the 'open association' model. In closed association, an increase in polymer concentration leads to the formation of more micelles of the same size. Micelle size in the systems is best

characterised by the mean number of hydrophobic groups per micelle. In open association, the size of the micelles or association structures increases with increasing polymer concentration. Open associations are characterised by the absence of a critical micelle concentration and the extent of aggregation is controlled by an equilibrium between single collapsed chains and aggregates of all sizes [26].

A single-coil to aggregate transition in the zinc salts of sulfonated polystyrene ionomers in xylene was studied by Bakeev and co-workers [27]. As the polymer concentration was increased in the dilute regime, the measured average diffusion coefficient of the polymer molecules decreased, and it was accompanied by a broadening in the distribution of the coefficient i.e. an increase in the aggregate size and polydispersity.

The concentration dependence of the apparent diffusion coefficient gives information about the interactions of the polymer with the solvent. The effect of the polymer concentration are considered by extrapolating the value of the apparent diffusion coefficient to zero concentration using the equation $D_{App}=D_0(1+k_Dc+\ldots)$ where k_D is the dynamic virial coefficient, c is the polymer concentration and D_0 is the diffusion coefficient at zero concentration. k_D can be related to the thermodynamic properties of the polymer/solvent mixture according to the equation $k_D=2A_2M-k_s-w$ where k_s is a friction term defined as $k_s=k_0(4\pi N_A/3)R_h^3/M$, w is the partial specific volume of the polymer in the solution, M is the molecular weight, A_2 is the second virial coefficient and k_0 a friction constant. This relationship is a result from linear irreversible thermodynamics [28] and has been tested in detail experimentally in dilute solutions by Brown and Zhou [29]. The first term ($2A_2M$) in the expression for k_D typically dominates in polymer solutions [29] and the slope obtained for the fast mode of the dilute PSS solutions indicates a slightly positive second virial coefficient and a situation of good solvent conditions, while the slope of the slow mode due to the aggregate is negative indicating a stronger attractive potential (Fig. 2).

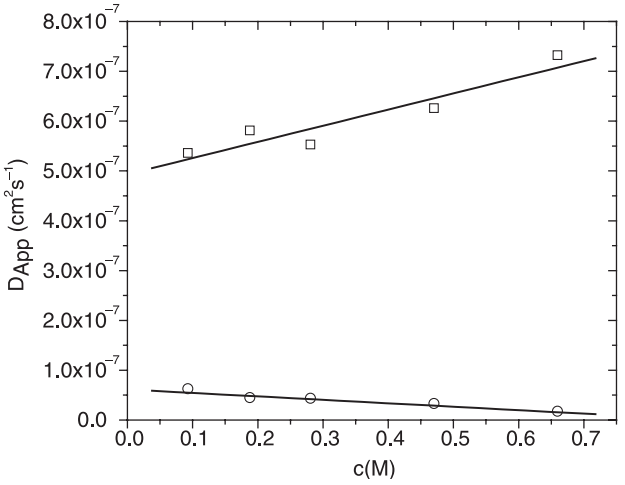

Fig. 2. Apparent diffusion coefficients (D_{app}) for PSS-Cs ($M_w=87{,}000$ g mol^{-1}) plotted against concentration to show the different slopes characterising the behaviour of (□) the single chain (positive second virial coefficient) and (○) the aggregate (negative virial coefficient).

3.2. SANS

In all the molecular weights of PSS-Cs examined in the dilute regime of polymer concentrations (0.0943 and 0.283 M) a standard Ornstein–Zernicke form of the scattering curve was obtained, while for higher concentrations an upturn of the curve is evident at low q (Fig. 3). Such an upturn is known as the Picot–Benoit [30] effect in semi-dilute solutions of neutral weakly associating polymers. The appearance of the excess scattering at low q with the strongly associating ionomers corresponds to the gelation point of the sample measured with rheology in the current study. Experimentally, such phenomena in semi-dilute solutions have sometimes been attributed to poor solution equilibration, but it also has been detected in carefully prepared homogeneous solutions. Guenet and co-workers [31] observe that in the case of polystyrene, the phenomenon depends on the nature of the solvent and there is a correlation between the occurrence of anomalous scattering and the potential for physical gelation at low temperature. With these weakly associating homopolymers the interpretation of the excess scattering is thus connected to the concept of macromolecule association in the form of aggregates.

Koberstein [32] found similar excess scattering for concentrated polystyrene solutions and the abnormal scattering is attributed to the presence of micro-domains of associated polymer in the solutions. We, therefore, considered the scattered intensity as the sum of two terms (Eq. (4)).

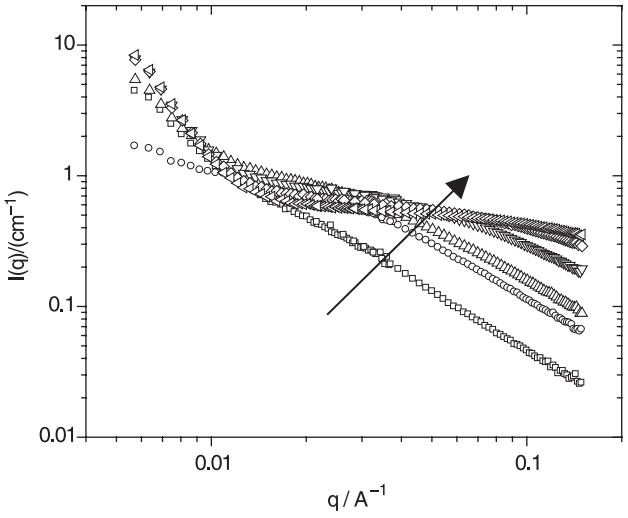

Fig. 3. SANS intensity as a function of q for the PSS-Cs ($M_w=87{,}000$) for increasing polymer concentration (0.0943–2.83 M). The excess scattering associated with gelation and phase separation becomes evident above a concentration of 0.47 M.

$$I(q) = \frac{I_1(0)}{(1 + q^2\xi^2)} + I_{ex}(q) \quad (4)$$

where ξ is the short-range screening length of the polymer mesh and I_{ex} is the low-angle excess intensity due to the long-range heterogeneities. However, we believe that in PSS ionomer samples the enhanced scattering is due to the dipole interaction of the charged groups causing micro-phase separation and gelation, a separate effect to that of Benoit and Picot with unsulphonated polystyrenes. The effect is evident in the case of concentrations above the overlap concentration (c^*); in the dilute regime the samples give a SANS curve typical of isolated polymer chains [33] (Fig. 3). However, as soon as the polymer concentration is above c^* the SANS curves are similar to those from type $1'+I$ chemically cross-linked gels [34]. Such scattering excesses in type $1'+I$ gels are attributed to frozen concentration fluctuations present in the gel on length scales that are larger than the blob size of the reference solution at the same concentration [11].

Although, the presence of the excess scattering makes calculation of the scattered intensity more complicated, it is still possible to calculate the small-scale correlation length (ξ) from the linear part of the $1/I(q)$ against q^2 plot (Eq. (4)). In this way, the correlation length of the samples was calculated for a range of polymer concentration using the Ornstein–Zernicke function [35]. The correlation lengths ξ obtained are plotted versus the concentration in Fig. 4(a). The concentration dependence of the correlation length follows a power law $\xi = 1.12c^{-0.72\pm0.03}$, where the exponent is slightly lower than the value -0.77 predicted from geometrical arguments [12] for semi-dilute solutions in a good solvent. Previously it was found that $\xi = 2.7c^{-0.72}$ for unsulphonated polystyrene in toluene [33]. The difference in the prefactor could be due to the higher concentration range in the current study where a strong entanglement of the polymer chains is involved. We deduce that the size of the correlation length corresponds to the distance between the polystyrene chains inside the micellar clusters (see the discussion of micro-phase separation which follows). The theoretical expression [11] for the correlation length of neutral polymer chains is

$$\xi \approx bc^{-\nu/(3\nu-1)} \quad (5)$$

where b is the Kuhn segment length, c is the monomer concentration and ν is a symbol dependent on the solvent quality. ν is equal to 0.59 for a good solvent and $\nu = 0.62$ in our case. An identical scaling is predicted for the correlation length of multisticker associating polymer solutions in agreement with our experiments [14].

The extrapolated forward scattering ($I_1(0)$) due to the small-scale mesh scattering was calculated as a function of concentration; $I_1(0) \sim Ac^{-0.33\pm0.07}$ and the exponent was again very close to the theoretical one of 0.31, expected for a semi-dilute polymer solution in a good solvent (we find $\nu = 0.58$ from this analysis). The theoretical expression for the forward scattering is [11]

$$I_1(0) \sim b_\nu^2 KTc^{\frac{3\nu-2}{3\nu-1}} \quad (6)$$

where b_ν is the scattering length contrast and kT is the thermal energy. The dependence of $I_1(0)$ on the polymer concentration is shown in Fig. 5.

We deduce that the small-scale structures of the polymer chains from the SANS data scales with polymer concentration exactly as expected for a semi-dilute solution of unassociating polystyrene chains in a good solvent. Such statistics are used in the model of Rubinstein and Semenov for associating micro phase separated polymers [14].

The excess scattering was examined as a function of concentration. We deduce that it is not due to the Picot–Benoit effect, since their model provides a poor fit of the data, and the opposite scaling to that predicted is observed for the second (large-scale) correlation length as a function of concentration [32]. Medjahdi and co-workers [36] attribute the Picot–Benoit effect to the existence of heterogeneities resulting from an attractive potential between the chains. The additional Debye–Bueche term, which they include in their model for $I_{ex}(q)$, is in good agreement with our data, but again the concentration dependence of the correlation length is incorrect. Furthermore, the model is inappropriate with ionomers since it assumes the charges (the attractive potential) are evenly distributed along the chain. We thus describe the intensity as a sum of two terms; the previous Ornstein–Zernicke term (Eq. (4)) and a Debye–Bueche term given by Eq. (7). Such a functional form of the scattered intensity is used to classify type $1'+I$ gels [11]. Ξ is the average thickness of the micro phase separated aggregate ($\Xi = (1/L_1 + 1/L_2)^{-1}$, (where L_1 and L_2 are the average thickness of the polymer and solvent rich phases) and $I_2(0)$ is the amplitude of the heterogeneity.

$$I_{ex}(q) = \frac{I_2(0)}{(1 + q^2\Xi^2)^2} \quad (7)$$

A good fit to the data is observed and it provides the correct trend of the correlation length on the polymer concentration i.e. the aggregates size increases with polymer concentration. The parameters $I_2(0)$ and Ξ were extracted by plotting $1/I_{ex}^{1/2}$ versus q^2 and a sample fit to the low q section of the data is shown in Fig. 4(b). A similar model has previously been used for compression molded random polystyrene ionomers in the solid state, although the polymer concentration could not be used as a parameter in this case [16].

We find the scaling of the large-scale inhomogeneities with polymer concentration of $\Xi = 24c^{0.58\pm0.05}$ and $I_2(0) \sim c^{2.0\pm0.4}$ (Figs. 4(a) and 5 inset). A schematic picture of the arrangement of the polymer chains deduced from the neutron and light scattering data is shown in Fig. 6. Note that the q^{-4} term in Eq. (7) corresponds to the scattering of a two-phase system and this is how we deduce the micro-phase separation shown in Fig. 6. Micro-phase separation is

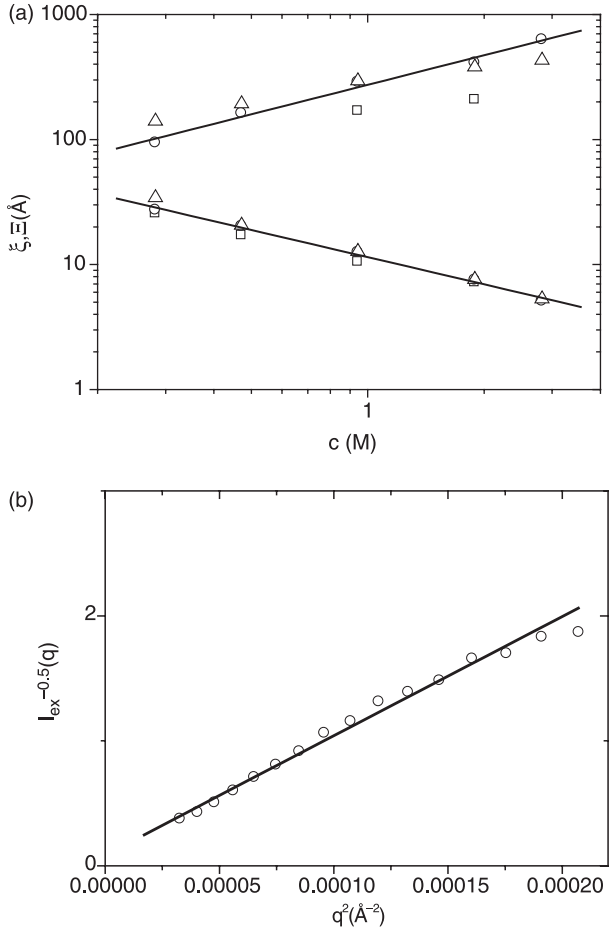

Fig. 4. (a) Scaling of the correlation lengths (ξ lower curve) and (Ξ upper curve) as a function of polymer concentration for different molecular weight. (□) $M_w = 55{,}000$ g mol^{-1}, (○) $M_w = 87{,}000$ g mol^{-1}, and (□) $M_w = 158{,}000$ g mol^{-1}. (b) Example of Debye–Bueche fit applied to the excess scattering I_{ex} to extract Ξ and $I_2(0)$.

predicted in the theory of Semenov and Rubinstein [14] for multiple sticker polymer solutions.

3.3. Bulk rheology

3.3.1. Linear viscoelasticity

The linear viscoelastic spectra of the ionomer solutions were fitted by a simple model of viscoelastic behaviour, the Maxwell model, corresponding to elastic and viscous components in series.

$$G'(\omega) = \frac{G_0\omega^2\tau^2}{1+\omega^2\tau^2}, \quad G''(\omega) = \frac{G_0\omega\tau}{1+\omega^2\tau^2} \tag{8}$$

where ω is the frequency (rad/s), G_0 is the plateau modulus, G' is the elastic modulus, G'' is the inelastic modulus and τ is the relaxation time. This simple model describes the data very well throughout the entire frequency range (Fig. 7).

Green and Tobolosky [37] first elaborated the basic theory of transient networks predicting a high-frequency storage modulus given by $G_0 = \nu kT$ where ν is the number density of elasticity effective chains, and a constant steady-shear viscosity of $\eta(\gamma) = \eta(0) = \tau G_0$ where the relaxation time τ is approximated as the reciprocal cross-over of the two moduli as the loss peak is not resolved in the experiment. The relaxation constant τ is shown as a function of concentration in Fig. 8. An unusual dependence of τ on polymer concentration is observed i.e. it decreases with increasing polymer concentration. The opposite trend is expected for non-associating polymer solutions and the internal dynamics of single sticky Rouse chains [13].

Relaxation times (τ) in the range 0.01–0.1 s are measured in the linear rheological studies. In the theory of Semenov and Rubinstein the slow dynamics are attributed to the process of micelle hopping and the correct dependence on the polymer concentration is predicted for the relaxation time [14]. Furthermore, the value of the plateau modulus can be considered in terms of how many chains contribute to the elasticity (kT per chain or aggregate of chains, Fig. 9). ν/n_c is the number of cross-links divided by the number of polymer chains. Such a calculation implies there are a wide range of 1–250 chains relaxing in a cluster at the terminal relaxation time [13] dependent on concentration and on chain length.

3.3.2. Shear viscosity

Polystyrene sulfonate ionomers are flexible chain macromolecules with widely spaced ionic groups that strongly attract each other. Solutions of these ionomers in non-polar solvents have unusual rheological properties. In contrast to non-associating polymer solutions, telechelic ionomers have been observed to exhibit shear thickening phenomenon [38]. To date randomly charged ionomers have not been studied in detail.

Shear flow is known to elongate polymers in solution. It seems reasonable that the elongation and alignment of the chains can increase the number of associations between chains, and thus create larger temporary complexes. It is known that polymers with higher degrees of polymerisation are more effective at increasing the viscosity than the small ones. Thus, shear flow can lead to increases in the viscosity.

In contrast, in our current experimental system, the PSS-thinning Cs samples show a novel step-like Bingham shear thinning [39]. A Newtonian (liquid-like) behaviour is observed in the high shear rate region and a critical shear stress (yield stress) was detected (Fig. 10). We believe that the micro-phase separated clusters of the dipolar groups (the long wavelength in homogeneities observed with SANS) are responsible for the structural arrest at low shear rates, creating a highly viscous associated fluid. This structure is subsequently ripped apart above a threshold stress corresponding to the cohesive energy of the micellar structures. The shear induces a macro-phase separation of the ionomer/solvent mixture into a high modulus viscoelastic fluid

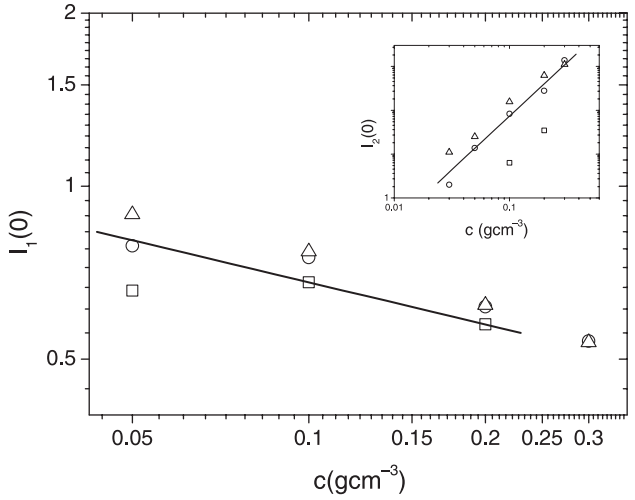

Fig. 5. The intensity of the excess scattering $I_1(0)$ calculated from a fit to the Ornstein–Zernicke function and $I_2(0)$ for Debye-Bueche (inset) plotted against concentration (M) for different molecular weight (△) M_w= 55,000 g mol^{-1}, (○) M_w=87,000 g mol^{-1}, and (△) M_w= 158,000 g mol^{-1}.

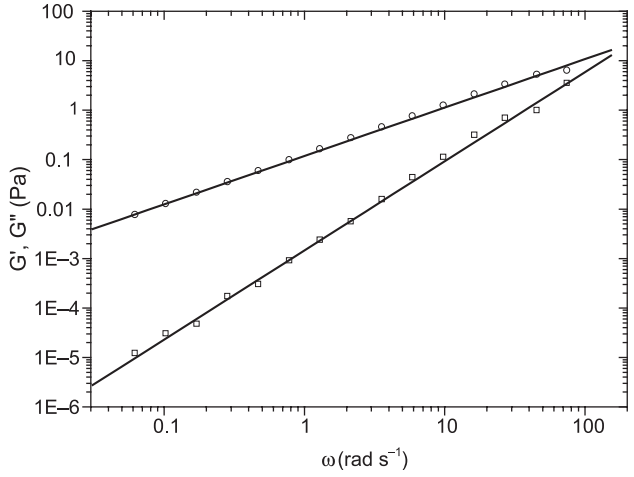

Fig. 7. Example of the rheology data obtained from linear oscillation experiments for PSS-Cs (M_w=158,000 g mol^{-1}) where the elastic modulus (□) and viscous modulus (○) are plotted as a function of frequency. The continuous lines are a fit to the Maxwell model.

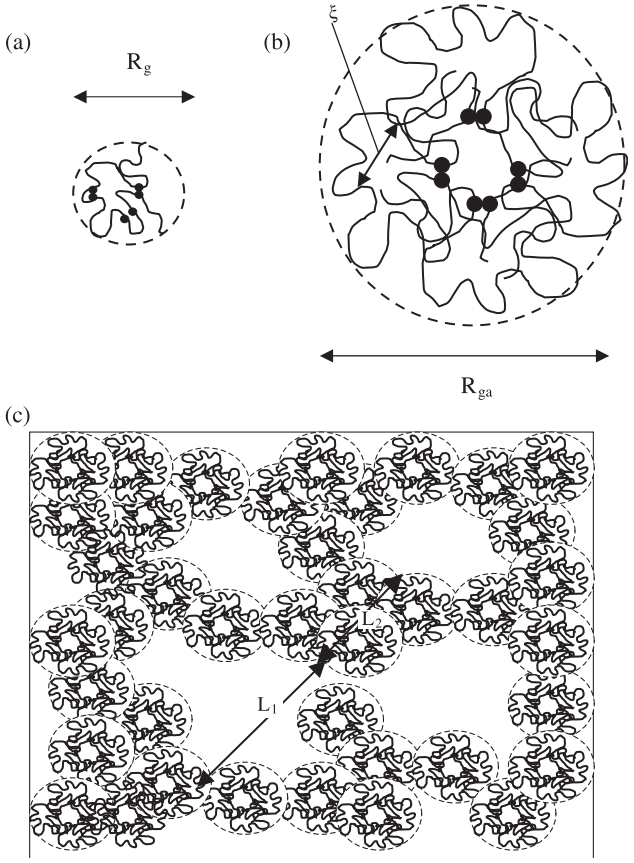

Fig. 6. Schematic picture representing the conformation of the ionomer chain (a) single chain with intra-chain interactions (radius of gyration R_g), (b) aggregates with both intra and inter chain associations (radius of gyration R_{ga}) and (c) phase separated gelled ionomer networks (correlation lengths $\Xi = (1/L_1 + 1/L_2)^{-1}$) [11].

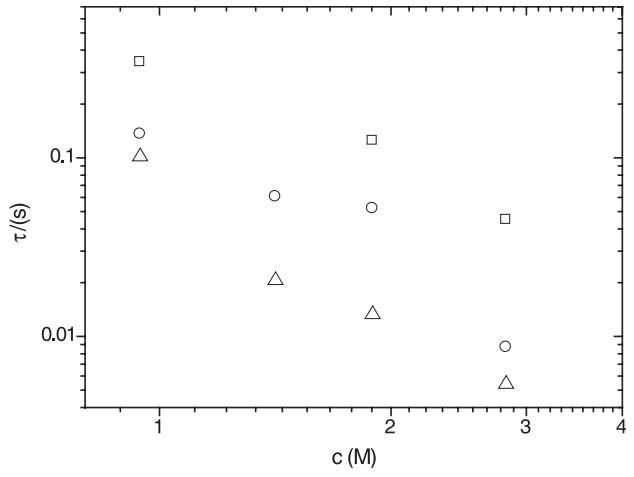

Fig. 8. The relaxation time plotted as a function of polymer concentration from fits with the Maxwell model for different molecular weights (□) $M_w = 55{,}000$ g mol^{-1}, (○) $M_w = 87{,}000$ g mol^{-1}, and (△) $M_w = 158{,}000$ g mol^{-1}.

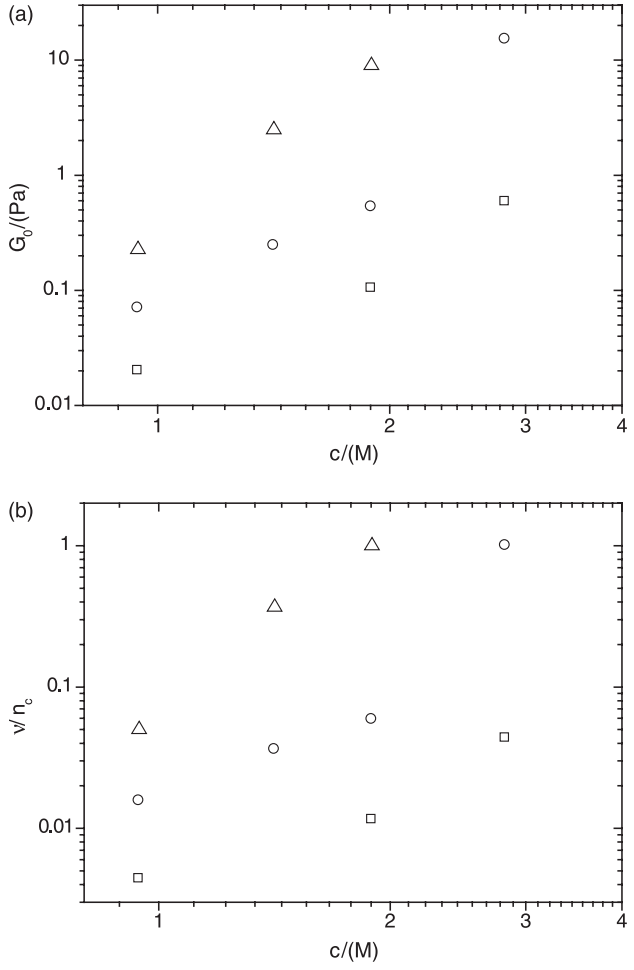

Fig. 9. (a) The plateau modulus and (b) the number of effective cross-links per chain responsible for the linear viscoelasticity (ν/n_c), plotted against concentration for ionomers of different molecular weights (□) $M_w = 55{,}000$ g mol^{-1}, (○) $M_w = 87{,}000$ g mol^{-1}, and (△) $M_w = 158{,}000$ g mol^{-1}.

interspersed with a solvent rich region resulting in a sudden reduction in the viscosity [40] as a function of shear rate.

The step like shear thinning of the ionomer solution is shown in Fig. 10. The yield stress increases with polymer concentration. Similar results were found for all the molecular weights studied. The time constant (τ_s) can be deduced from the sharp change in the viscosity as a function of the shear rate.

This is situated at about 6–10 s^{-1}which gives a τ_s of 0.1–0.15 s. This time constant is of the same order of magnitude as that attributed to the dynamics of micelle hopping in the linear viscoelastic data from the Semenov and Rubinstein [14] model.

4. Conclusions

Dynamic light scattering, small angle neutron scattering and bulk rheology can be used to characterise the sticky dynamics of random polystyrene caesium sulphonate ionomers. In the dilute regime, DLS allowed measurement of both the hydrodynamic radius of the single chain and the aggregates formed by dipolar interaction of the charged groups. Using SANS the evolution with polymer concentration of the structure of the micro-phase separated aggregates was measured. Two correlation lengths of the network have been calculated using the Ornstein–Zernicke fit at small length scales (the mesh size) and a Debye–Bueche fit at large length scales (micro-phase separated aggregates).

From the scattering data we deduce that the associating ionomers in solution at low concentrations form flowerlike micelles consisting of looped chains in which charged groups are located in the core of the micelle [14]. As the polymer concentration increases, a secondary association

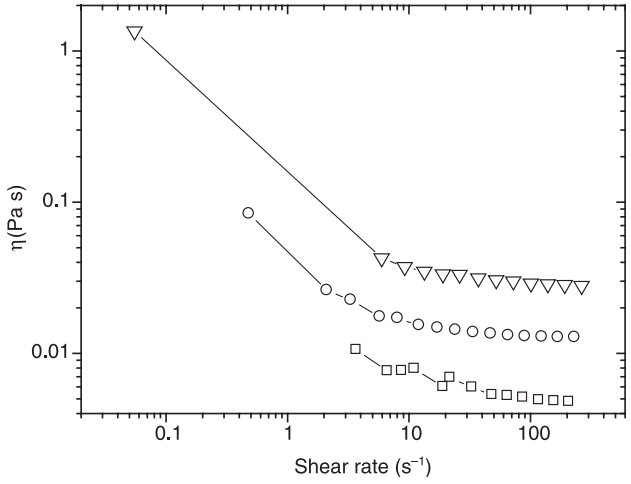

Fig. 10. Viscosity of PSS-Cs with molecular weights $M_w = 87{,}000$ g mol^{-1}. The phase separation of the system is clearly shown by the drastic step like decrease of η with a characteristic yield stress. The symbols indicate the different polymer concentrations; (□) 0.941 M, (○) 1.89 M, and (△) 2.83 M.

process occurs leading to the formation of bridges between micelles, until finally a network is formed with a large increase in viscosity. Micro-phase separation between a dilute solution of separated micelles and a dense phase of aggregated micelles is observed at high polymer concentrations causing the excess scattering at large length scales in SANS experiments. The behaviour of the micro-phase separation depends strongly on the length of the polymer backbone.

The rheology showed that the samples follow a Maxwell model with a single relaxation constant at low frequencies. The modulus indicates that ionomer chains assembled into many chain clusters are responsible for the viscoelasticity at the terminal relaxation time. The relaxation time decreases with polymer concentration as predicted with models of stress relaxation through a micellar hopping process [14].

A shear induced macro-phase separation provides a step like shear thinning (Bingham) behaviour with the solutions. At high shear rates the clusters are fragmented, do not have the time to aggregate and are thought to form a macro-phase separated fluid. Below a certain critical shear rate the ionomer solutions are able to form bridges between micellar clusters that transform the material into a viscoelastic network.

Acknowledgements

This work is supported by the EPSRC. We also thank Professor Eric Dickinson and Miss Helen Babin (Food Science Department) for the use of the rheometer. The article's referees are thanked for their insightful comments.

References

[1] Pedley A, Higgins J, Peiffer D, Rennie A. Macromoleules 1990;23: 2494–500.
[2] Eisenberg A, King M. Ion-containing polymers: physical properties and structure. New York: Academic Press; 1977.
[3] Eisenberg A, Kim J. Introduction to ionomers. London: Wiley; 1998.
[4] Lundberg R, Phillips R. J Polym Sci Polym Phys 1982;20:1143–54.
[5] Lundberg R. J Appl Polym Sci 1982;27:4623–35.
[6] Lundberg R, Phillips R. J Polym Sci Polym Phys 1989;27:245–60.
[7] Pedley A, Higgins J, Peiffer D, Burchard W. Macromolecules 1990; 23:1434–7.
[8] Lantman C, Macknight W, Higgins J, Peiffer D, Sinha S, Lundberg R. Macromolecules 1988;21:1339–43.
[9] Lantman C, Macknight W, Peiffer D, Sinha S, Lundberg R. Macromolecules 1987;20:1096–101.
[10] Chakrabarty K, Seery TA, Weiss RA. Macromolecules 1998;31: 7385–9.
[11] Bastide J, Candau SJ. Structure of gels as investigated by means of scattering techniques. In: Addad JPC, editor. The physical properties of polymeric gels. New York: Wiley; 1996.
[12] Daoud M, Cotton JP, Farnoux B, Jannink G, Sarma G, Benoit H, et al. Macromolecules 1975;8:804–18.
[13] Rubinstein M, Semenov AN. Macromolecules 2001;34:1058–68.
[14] Semenov AM, Rubinstein M. Macromolecules 2002;35:4821–37.
[15] Rubinstein M, Colby RH. Phys Rev Lett 1994;73(20):2776–9.
[16] Li Y, Peiffer DG, Chu B. Macromolecules 1993;26:4006–12.
[17] Mallam S, Hecht AM, Geissler E, Pruvost P. J Chem Phys 1989;91: 6447–54.
[18] Zielinsky F, Buzier M, Lartigue C, Bastide J, Boue F. Prog Colloid Sci 1992;90:115–30.
[19] Meins JL, Tassin J. Macromolecules 2001;34:2641–7.
[20] Migler K, Liu C-H, Pine DJ. Macromolecules 1996;29:1422–32.
[21] Makowski HS, Lundberg RD, Singhal GL. US Patent 870841; 1975.
[22] Provencher S. Comput Phys Commun 1982;27(3):229–42.
[23] Bodycomb J, Hara M. Macromolecules 1995;28:8190–7.
[24] Grosberg AY, Khokhlov AR. Statistical physics of macromolecules. New York: AIP Press; 1994.
[25] Appelt B, Meyerhoff G. Macromolecules 1980;13:657–62.
[26] Elias HG. In: Light scattering from polymer solutions. New York: Academic Press; 1972.
[27] Bakeev K, Teraoka I, Macknight W, Karasz F. Macromolecules 1993; 26:1972–4.
[28] Yamakawa HY. Modern theory of polymer solutions. New York: Harper and Row; 1971. p. 242.
[29] Brown W, Zhou P. Macromolecules 1991;24:5151–7.
[30] Benoit H, Picot C. Pure Appl Chem 1966;12:545–61.
[31] Guenet J, Wilmoth N, Ellsmore P. Polym Commun 1983;24:230–3.
[32] Koberstein J, Picot C, Benoit H. Polymer 1985;26:673–81.
[33] Brown W, Mortensen K, Floudas G. Macromolecules 1992;25: 6904–8.
[34] Mendes E, Lutz P, Bastide J, Boue' F. Macromolecules 1995;28: 174–9.
[35] Ornstein LS, Zernicke F. Proc Acad Sci Amsterdam 1914;17:793.
[36] Medjahdi G, Sarazin G, Francois J. Macromolecules 1991;28: 4138–41.
[37] Green M, Tobolsky A. J Chem Phys 1946;14:80–9.
[38] Yekta A, Xu B, Duhamel J, Adiwidjaja H, Winnik M. Macromolecules 1995;956–66.
[39] Macosko CW. Rheology principles, measurements and applications. New York: VCH Publisher Inc; 1994.
[40] Olmsted PD. Curr Opin Colloid Interface Sci 1999;4(2):95–100.